



Petroleum refinery wastewater degradation by heterogeneous-electro-fenton process using activated carbon loaded with Iron and Cerium: A kinetic study

Asyah R. Flayyih ^{a,*}, Wadood T. Mohammed ^a, Ali H. Abbar ^b

^a Department of Chemical Engineering, College of Engineering, University of Baghdad, Baghdad, 10071, Iraq

^b Department of Biochemical Engineering, Al-Khwarizmi College of Engineering, University of Baghdad, Baghdad, 10071, Iraq

Abstract

This work aims to study the kinetics of heterogeneous electro-Fenton (HEF) process used to treat petroleum refinery wastewater by a catalyst made of an activated carbon loaded with iron and cerium. Effects of HEF operating variables such as current density, dose of catalyst, and pH on the removal of COD and reaction rate constant (k_{app}) were examined. Results showed that decline of COD with time at different operating conditions obeys a pseudo-first-order kinetics with a regression fitting (R^2) not less than 0.97. Furthermore, increasing the current density was found to give higher rate of COD removal and k_{app} to a limit beyond which no longer enhancement can be achieved. Similar behaviour regarding to the dose of catalyst while increasing pH has an adverse effect. The best operating conditions that give high rate of COD removal and k_{app} were a current density of 10 mA/cm², a dose of catalyst equal to 1.0 g/L, and a pH of 3, in which 86.97% of COD was removed with k_{app} value equal to 0.0188538 min⁻¹ which required only 13.06 KWh/kg COD as an electrical energy consumption. The present system approved to have high reaction rate and could be applied to treat various types of wastewaters.

Keywords: petroleum refinery wastewater; pseudo first order kinetics; heterogeneous electro-Fenton; Advanced oxidation process.

Received on 18/10/2025, Received in Revised Form on 25/01/2026, Accepted on 25/01/2026, Published on 30/03/2026

<https://doi.org/10.31699/IJCPE.2026.1.3>

1- Introduction

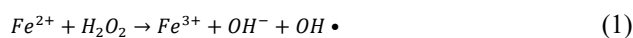
Water is very important for life and human beings, and its availability is the main task of all industrial sectors [1]. However, a large amount of wastewater is generated from these sectors and disposed of without a proper management or treatment [2]. Petroleum refinery is one such sectors that has generated a huge amount of wastewater and faces treatment difficulties to discharge these effluents in a safe manner [3]. Refinery wastewater contains various organic and inorganic compounds, including phenols, hydrocarbons, sulfides, and heavy metals making it very dangerous to the aquatic system [1, 3]. Various types of treatment methods have been applied for petroleum refinery wastewater, including biological, chemical, and physical methods [4-10]. However, these methods are inefficient, unable to decompose the recalcitrant organic compounds, generate a large amount of sludge, and require a large and expensive space [4, 5].

Advanced oxidation processes (AOPs) are other technologies with a basic toolkit that enables them to degrade a variety of organic contaminants [11]. These processes produce highly reactive $\cdot\text{OH}$, which rapidly oxidizes organic contaminants, converting them to less harmful molecules, most precisely to carbon dioxide and water [12]. In general, AOPs include the Fenton reaction, ozonation, and UV/H₂O₂ methods. These methods have

the potential to increase the efficiency of petroleum refinery wastewater treatment by removing refractory or non-biodegradable contaminants that are difficult to remove with the conventional methods, providing cleaner and safer discharges to the environment [3, 13].

Electrochemical advanced oxidation processes (EAOPs) are among the most widely used groups of advanced oxidation processes in industrial wastewater treatment [14]. These technologies are characterized by their low cost, high removal rate, ease of operation and scale-up, and no generation of secondary toxic pollutants [15]. These processes include anodic oxidation (AO), electro-Fenton (EF), sonoelectro-Fenton, and photoelectro-Fenton [16-22].

EF, one of the well-known EAOPs, can produce a strong oxidizing agent ($\cdot\text{OH}$), with a standard electrode potential of 2.8 V/SHE, via the Fenton reaction (Eq. 1), thereby degrading most pollutants in PRW [23].



Where H₂O₂ is produced via reducing O₂ supplied from air/oxygen at the cathode (Eq. 2):



*Corresponding Author: Email: asiyah.falih2207d@coeng.uobaghdad.edu.iq

© 2026 The Author(s). Published by College of Engineering, University of Baghdad.

This is an Open Access article licensed under a [Creative Commons Attribution 4.0 International License](https://creativecommons.org/licenses/by/4.0/). This permits users to copy, redistribute, remix, transmit and adapt the work provided the original work and source is appropriately cited.

Based on the properties of the catalyst involved in this process, EF can be divided into homogeneous and heterogeneous processes [24, 25]. In conventional homogeneous EF, the catalyst is an externally added soluble iron salt that is ionic in the solution, making it difficult to separate and recycle, resulting in the generation of a large amount of iron sludge as the solution pH is adjusted to a neutral value [26]. This, in turn, increases the operating cost. Furthermore, homogeneous EF suffers from low H₂O₂ generation rate, low current efficiency, a narrow pH operating range (2-4), and a long reaction time [27]. Compared with the homogeneous type, heterogeneous electro-Fenton (HEF) has many advantages such as catalyst reusability, working near neutral pH, low cost, and long service life [28]. Accordingly, the selection of a suitable catalyst has become a new research focus. Various types of HEF catalysts have been used such as chalcopyrite [29], pyterite [30], Fe-based bimetallic catalyst [31], and α -FeOOH [32]. Among which zero-valent iron catalysts are the best due to their low cost, strong reducing ability, and good performance [33–36].

However, these catalysts are difficult to handle or store due to their aggregation property [37]. Therefore, they are preferably supported on activated carbon to solve this problem [38, 39].

Studying the kinetics of EAOPs offers numerous advantages from both an economic and engineering perspective. Kinetic data provide insight into the rate of contaminant degradation under specific operating conditions, enabling the identification of optimal EAOPs based on high removal rates and low energy consumption. Furthermore, kinetic parameters are important for scaling up a system from a laboratory scale to a pilot plant scale and then to an industrial scale, providing a basis for determining reactor size, operating time, and electrode surface area. Kinetic analysis prevents overtreatment by stopping the process at the point of diminishing returns, by linking the degradation rate to the specific energy consumption [40]. In the EAOPs, specifically electro Fenton and heterogeneous electro Fenton, kinetics of Fenton reactions happened during the process are very complex due to involve a large number of reaction steps that performed simultaneously and not macroscopically detectable [41]. It was found that in these processes, the oxidation of organic pollutant as well as their by-products is performed by \cdot OH radicals attacking, and reaction rate can be expressed by the following equation in terms of COD as a concentration of pollutants [42-46]:

$$r = \frac{dCOD}{dt} = k[HO^{\cdot}]^{\alpha} COD \quad (3)$$

In Eq. 3; k represents the reaction rate constant, α is the reaction order of hydroxyl radicals' concentration, However, the ratio of the COD to \cdot OH was low and the concentration of \cdot OH radicals can be considered constant. In this case Eq. 3 can be written as follows:

$$r = \frac{dCOD}{dt} = k_{app} COD \quad (4)$$

Where $k_{app} = k[HO^{\cdot}]^{\alpha}$ represents the apparent rate constant. The integration of Eq. 4 subject to the initial conditions $COD=COD_0$ at $t=0$ leads to the following equation:

$$COD = COD_0 \exp(-k_{app}t) \quad (5)$$

This equation is termed as a pseudo first order kinetic in which k_{app} is known as a pseudo-first-order kinetic constant which could be calculated from the plot of $\ln(COD_0/COD)$ versus t [47].

Many kinetics studies have been reported for treating various organic pollutants using heterogeneous electro-Fenton process [23, 41, 42, 48-53]. However, studying the kinetic of COD removal from petroleum refinery wastewater using AC loaded with Fe+Ce in a HEF process was not reported previously. AC loaded with Fe+Ce was found by our previous work [54] has good catalytic activity in removal of methylene blue due to the incorporating CeO₂ with Fe@Fe₂O₃ which played an essential role since CeO₂ has large amount of oxygen vacancy defects resulted from the redox conversion between Ce⁴⁺ and Ce³⁺ causing more activating of H₂O₂ to generate more \cdot OH radicals during the process [55].

Therefore, the aim of this study is to examine the kinetic of COD removal by AC loaded with Fe+Ce as HEF catalyst using a new design of electrochemical reactor consisting of cheap electrodes and easy to scale-up. Impacts of operating factors such as current density, dose of catalyst, and pH on the removal rate of COD and pseudo first order kinetic rate constant were investigated.

2- Materials and method

2.1. Chemicals

Commercial activated carbon (AC) was purchased from Zhengzhou Kelin Company, China. It has the following specifications: total surface is 950-1200 m²/g, apparent density 460±40kg/m³, ash content 5%, moisture content 8%. Sodium borohydride (NaBH₄, ≥99%) was purchased from Fluka-Garantie. FeCl₃·6H₂O with a purity of 97% was purchased from Loba Chemie PVT Ltd, India. Ce(NO₃)₃·6H₂O with a purity of 98% was purchased from Himedia Laboratories Pvt.LTD, India. Acetone, ethanol, Na₂SO₄, HCl, and NaOH were analytical grade and used without needing for purification. All runs were performed using distilled water with a conductivity of 0.05 μS/cm.

The performance of the AC catalyst loaded with Fe/Ce (2:1) in COD removal from petroleum refinery wastewater generated at Al-Dora refinery plant located at Baghdad province, Iraq was evaluated using the heterogeneous EF. The wastewater had the characteristics listed in Table 1.

2.2. Synthesis of AC loaded Fe/Ce

Synthesis of the catalyst was performed according to our previous work [54]. Firstly, 20g of AC was sieved, and the cut of 40 to 60 mesh was isolated and used in

preparing the catalyst. The isolated amount was soaked in 5% HCl for 24 h, washed with distilled solution, filtered, followed by measuring the pH of filtrate. This cycle was repeated several times until the pH of the solution reached 6.5–6.7. The washed AC was dried at 105 °C for 24 h and stored until used as a support material. The composite Fe@Fe₂O₃ and CeO₂ were loaded onto AC as follows:

Appropriate amounts of FeCl₃·6H₂O and Ce (NO₃)₃·6H₂O were dissolved in 100 mL of a 30/70, v/v, ethanol-water mixture at pH 4. The prepared solution had a total concentration of 0.07 M for Fe+Ce. Then, 4 g of AC was added to the above solution, and the resulting solution was mixed for 60 min at room temperature and 500 rpm. 50 mL of 0.5 M NaHB₄ was prepared and added dropwise (2 mL/min) to the AC-containing solution, mixing for another 30 min. The resulting catalyst was filtered, washed with ethanol and distilled water three times each, and dried at 70 °C for 6 h.

2.3. Electrochemical system

The heterogeneous EF system consists of an electrochemical cell, a power supply UNI-T, UTP3315TFL-II, China), an overhead stirrer (Heidolph

overhead stirrer company, Germany), an air pump (HAILEA, Aco-318, China), an Ammeter (UNI-UT39C⁺, China), and an air flow meter (Flowtech-z-7002, China).

The heterogeneous EF system is based on an electrochemical cell with a novel design. It consists of a cell body and its cover, a microporous air diffusion cathode, and a porous graphite anode. The cell body is a cylindrical Perspex vessel (outer diameter = 90 mm, inner diameter = 80 mm, length = 160 mm), while its cover is a disc made of the same material (outer diameter = 120 mm, thickness=10 mm) enclosed inside the cell body. The cover has three silt: a central silt (40 x 20 mm), a slit for inserting the cathode (40 x 15 mm), and a slit for inserting the anode (40 x 5 mm). The gap between the anode and cathode was fixed at 25 mm. The anode is a porous graphite plate (150 x 40 x 4 mm). The air-diffused cathode consists of two parts: a graphite plate and a Perspex brood cavity. The graphite plate (139 x29 x 4 mm) was machined with 300 μm holes with a total of 60 holes, which are evenly distributed at the lower section of the graphite plate (60 x 30 mm). While the rectangular brood cavity has dimensions (150 x 40x 15 mm), Fig. 1 shows the schematic of the heterogeneous EF system.

Table 1. Characteristics of wastewater

Characteristic	pH	TDS	Phenol	COD	BOD	Oil	Cl ⁻	Turbidity
Value	6.6	ppm	18.5 ppm	307 ppm	140 ppm	20.2 ppm	840 ppm	35 NTU

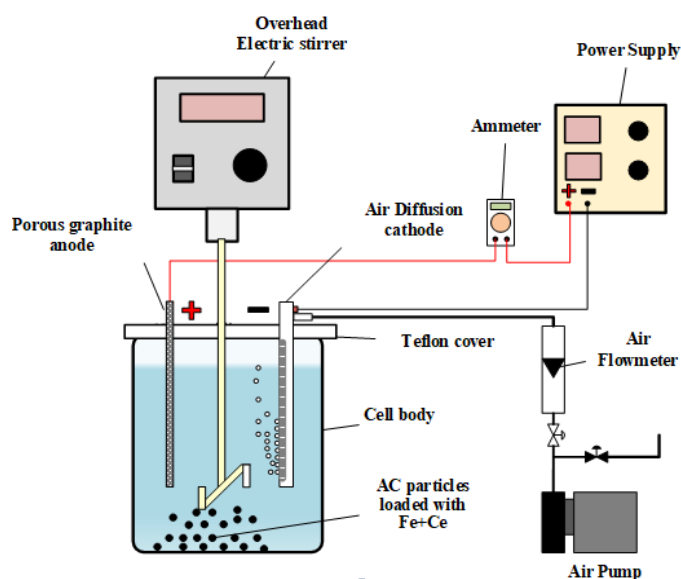


Fig. 1. Schematic of the heterogeneous EF system

2.4. Analysis and measurements

The crystalline structure and morphology of prepared catalyst was examined using X-ray diffraction (XRD) device, Panalytical X'pert Pro, Netherlands and scanning electron microscopy (SEM) device, Czech Republic.

Lovibond thermo-reactor was utilized to measure the COD via heating up the reagents to 150 °C for 2 hours. Turbidity was measured by the turbidity meter-TB 210 IR Lovibond, Germany. The removal efficiency of COD or

any phenolic compound can be evaluated based on Eq. 6 [44]:

$$RE\% = \frac{C_i - C_f}{C_i} \times 100 \quad (6)$$

Where C_i stands for the initial concentration (mg/L), C_f stands for the final concentration (mg/L), and RE% stands for removal efficiency.

The specific energy consumption (SEC) for treatment process was calculated using Eq. 7 [45]:

$$SEC = \frac{U \cdot I \cdot t \cdot 1000}{(COD_0 - COD_f) \cdot V} \quad (7)$$

Where SEC stands for specific energy consumed (kWh/kg COD), U, for cell voltage (Volt), I, for current intensity (A), t, for time (h), V, for water volume (L), COD_0 and COD_f are the initial and final chemical oxygen demands (mg/L). The operating variables and their ranges used in the present work is illustrated in Table 2.

Table 2. Operating variables and their range

Variable	Range
Current density(mA/cm ²)	5,10,15
pH	3,6,9
Dosage of catalyst (g/L)	0.5,1,1.5

3- Results and discussion

3.1. Characterization of the catalyst

To demonstrate the success of loading process for the activated carbon, XRD and SEM tests were performed as shown in Fig. 2 and Fig. 3. Fig. 2 displays XRD results for the prepared catalyst where no sharp peak can find at 2θ values between 20° and 30° confirming amorphous structure of carbon [55]. A clear peak of zero valent iron was observed at 2θ of 44.7° (JCPDS, NO. 06-0696) [56, 57]. While peaks of Fe_2O_3 was observed at 2θ of 35.6° (JCPDF, NO. 89-0691) [58]. Two peaks of CeO_2 were detected at 2θ of 33.32° , 56.76° (JCPDF, NO. 34-0394) [58, 59].

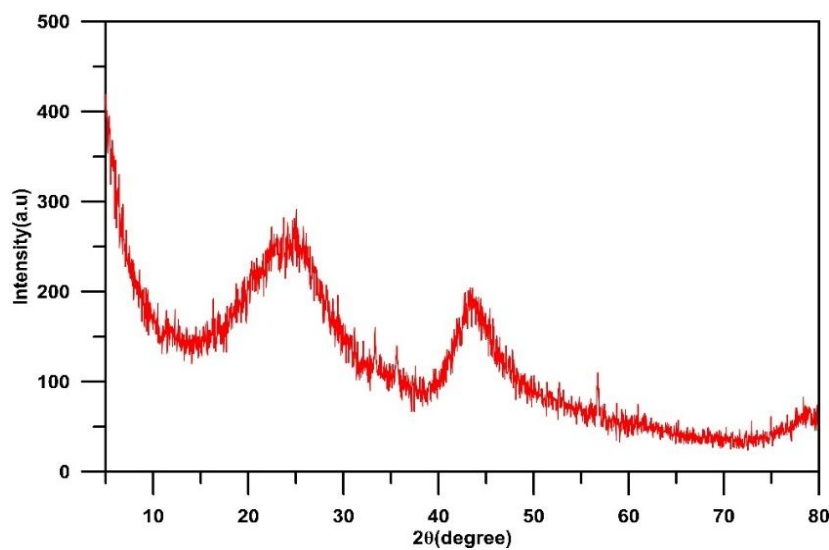


Fig. 2. Shows SEM of catalyst where results showed good immobilized of zero-valent and cerium oxide within the latex of AC. Similar observation were noted in previous works [60]

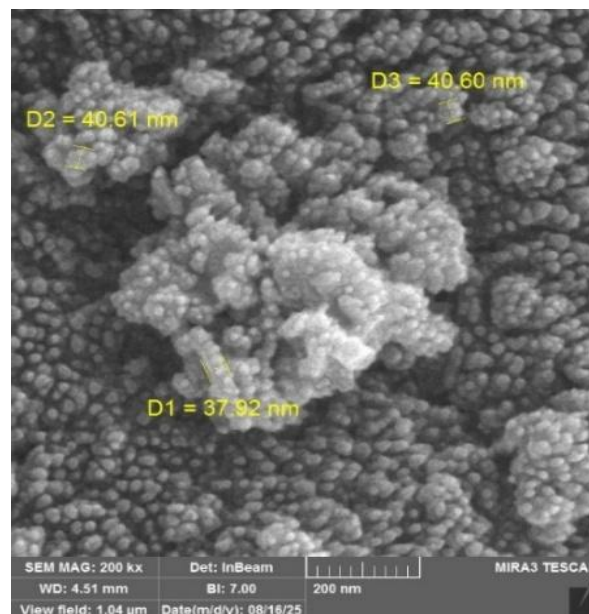


Fig. 3. SEM of the catalyst

3.2. Effect of operating variables

3.2.1. Effect of current density

Fig. 4 displays the decay in COD with time at different current densities for operating time of 120 min at constant catalyst dose (1 g/L) under initial pH of 6, while Fig. 5 represents the corresponding plot of $\ln(\text{COD}/\text{COD}_0)$ versus time. The results show that the decrease in COD with time exhibits an exponential behavior, while a straight linear relationship was found for $\ln(\text{COD}/\text{COD}_0)$ with time, confirming pseudo first-order kinetics. Also increasing current density results in increasing COD removal to a maximum value beyond which start to decrease with further increasing in its value where a maximum removal efficiency of 84.5% was obtained at a current density of 10 mA/cm² as shown in Table 3. In fact, increasing current would accelerate the formation of H₂O₂ on the cathode according to Eq. 2 and activating the oxidation power of the catalyst to generate further •OH radicals [61]. Also, at the same time, regeneration of Fe²⁺ by reduction of Fe³⁺ on the cathode (Eq. 8) increases with increasing current density leading to more degradation of COD [48].



Conversely, high current density could lead to reduce the rate of H₂O₂ generation due to parasitic reactions (reducing O₂ to H₂O instead of H₂O₂ (Eq. 9) and H₂ generation (Eq. 10) occurred on the cathode [62]:



Table 3 shows the value of k_{app} at different current densities, with the corresponding regression coefficient (R²) having values above 0.980. At 5 mA/cm², k_{app} was 0.01508 min⁻¹ which increased to 0.01738 at 10 mA/cm² leading to an increment of 20% in its value. However, k_{app} decreased by 10% in further increasing of current density. Thus, increasing the current density improves the reaction rate to a maximum value beyond which it is not recommended to further proceed the reaction. Table 3 displays that increasing the current density led to increase the electrical energy consumption and a current density of 10 mA/cm² is preferred in terms of lower energy consumption with higher removal of contaminants.

A similar observation regarding the effect of current density on k_{app} was confirmed by Pormazar and Dalvand [41] in the degradation of DB80 dye using HEF with Fe₃O₄ magnetite-loaded AC. Xu et al. [23] found that the maximum reaction rate constant (0.0201/s) was obtained at a current density of 5 mA/cm², which then decreased with further increase in current density during the treatment of a polyacrylamide contaminant using HEF with CoFe₂O₄ catalyst. Tan et al. [48] also found that increasing the current density from 10 to 30 mA/cm² resulted in a significant enhancement in the kinetic

constant from 0.0244 to 0.12 min⁻¹. However, it subsequently decreased with increasing current density during the treatment of Rhodamine B by HEF with nano-calcined pyrite.

3.2.2. Effect of Catalyst dosage

Fig. 6 shows the decay in COD with time at different catalyst dosages for operating time of 120 min at 10 mA/cm² and initial pH of 6. While Fig. 7 denotes the corresponding plot of $\ln(\text{COD}/\text{COD}_0)$ versus time. Similarly, the decrease in COD with time was found to follow an exponential behavior, and a straight linear relationship for $\ln(\text{COD}/\text{COD}_0)$ with time was observed approving pseudo first-order kinetics for COD removal from PRW. The results show that increasing the catalyst dosage would enhance the COD removal and rate constant to a maximum value after which the removal rate and reaction rate constant decrease for further increase in the catalyst dosage. The increase in both COD removal and k_{app} with increasing in dose of catalyst up to 1g/L could be interpreted by the increase in number of active sites as catalyst quantity increased, favoring more H₂O₂ reaction to generate more reactive oxidant (HO•) [62]. The decrease in both COD removal and k_{app} as the dose of catalyst exceeded 1 g/L can be explained by the reaction of Fe²⁺ with HO• (Eqs. 11 and 12) as well as the side reactions (Eqs. 13 and 14) resulted from HO• reactions [48, 63, 64].

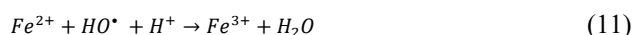


Table 4 shows the K_{app} value at different catalyst dosages, with the corresponding R² values exceeding 0.979. At 0.5 g/L, the K_{app} value was 0.01350 min⁻¹, and it increased to 0.01738 min⁻¹ at 1.0 g/L, resulting in a 29% increase in its value. However, the K_{app} value decreased by 11% with increasing catalyst dosage. Therefore, increasing the catalyst amount improves the reaction rate to a maximum value beyond which it is no longer recommended to continue the reaction from economic and recycling aspects. Table 4 shows that increasing the catalyst dosage has a slightly effect on electrical energy consumption.

Similar behaviors have been reported in previous studies; for example, Tesnim et al. [38] found that increasing the AC-NZVI dosage from 0.8 to 1.4 g/L increased pseudo-first order rate constant from 0.87 to 1.73 min⁻¹, with a slight decrease as the catalyst dosage reached 1.6 g/L during the treatment of wastewater containing an antipyrene via HEF using AC-NZVI. In another study conducted by Xu et al. [23], the pseudo-first order rate constant increased from 0.0112 to 0.0256/s with an increase in the CoFe₂O₄ catalyst dosage from 0.1 to 0.4

g/L during the treatment of a polyacrylamide contaminant using HEF. However, they found that increasing the catalyst dosage above 0.4 g/L resulted in a negligible improvement in the reaction rate constant. Tan et al. [48] observed that increasing the catalyst dosage from 0.5 to 1.0 g/L increased the rate constant by 1.55 times.

However, the rate constant decreased with increasing catalyst amount beyond 1.0g/L during the treatment of Rhodamine B by HEF using calcined nanopyrite. Sadeghi et al. [52] observed a similar trend during the degradation of diclofenac by HEF using a catalyst made of magnetic single-walled carbon nanotubes.

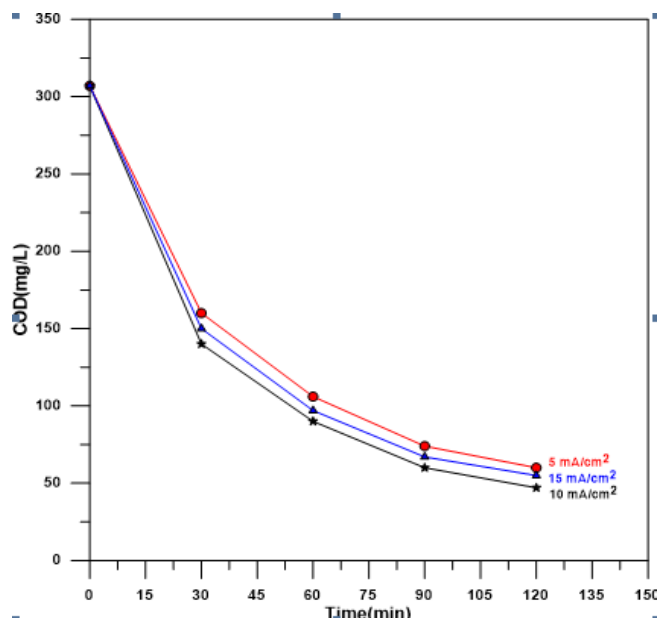


Fig. 4. Effect of the current density on the COD removal in HEF

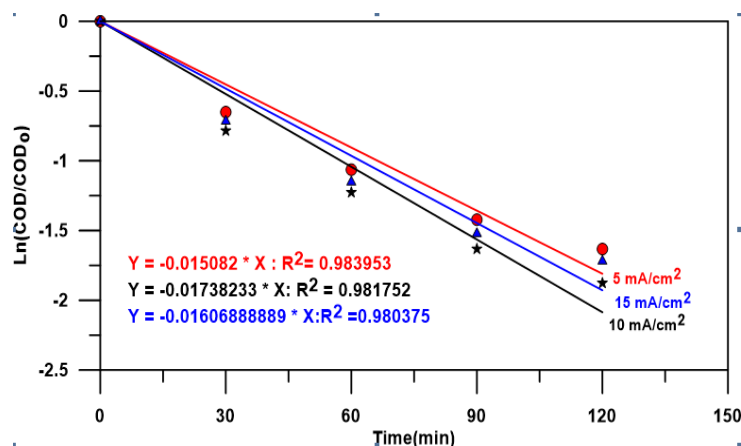


Fig. 5. Pseudo-first order kinetics for different current density at HEF. pH=6, 1g/L catalyst

Table 3. Apparent rate constant at different current densities

Current density (mA/cm ²)	Final COD (mg/L)	RE%	SEC (KWh/ kg COD)	K _{app} (min ⁻¹)	R ²
5	60	80.45	5.52	0.01508	0.983953
10	47	84.5	13.38	0.01738	0.981752
15	55	82.08	24.83	0.01607	0.980375

Table 4. Apparent rate constant at different catalyst dosage

Dosage (g/L)	Final COD (ppm)	RE%	SEC (KWh/ kg COD)	K _{app} (min ⁻¹)	R ²
0.5	73	76.22	15.12	0.01350	0.979540
1.0	47	84.50	13.38	0.01738	0.981752
1.5	53	82.74	14.70	0.01558	0.980793

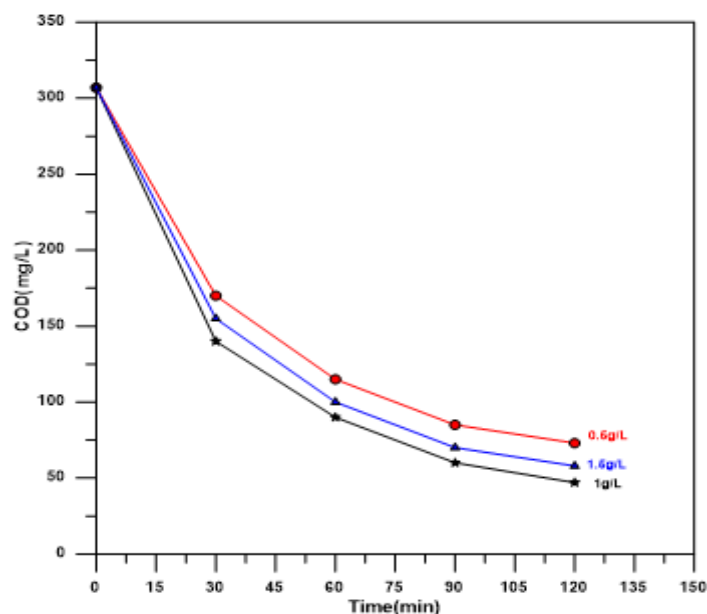


Fig. 6. Effect of catalyst dosage on the COD removal

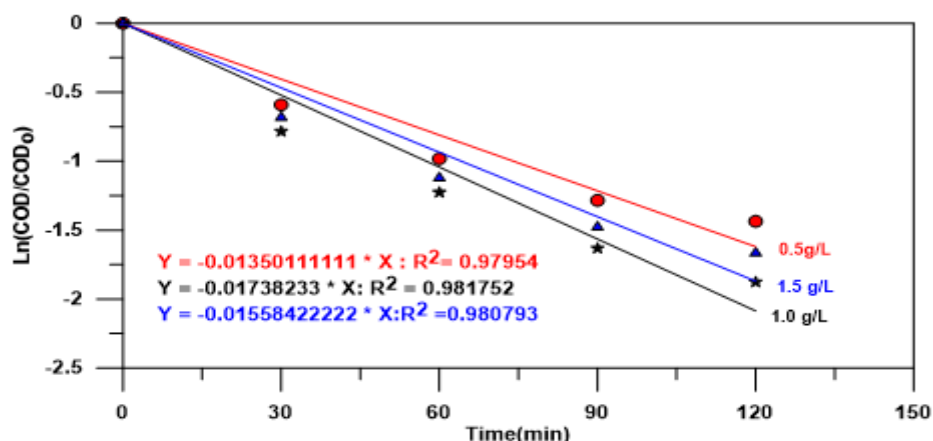


Fig. 7. Pseudo-first order kinetics for different catalyst dosage at HEF. pH=6, 10 mA/cm²

3.2.3. Effect of Ph

PH plays a vital role in controlling the activity of the catalyst, the activities of oxidants and substrates, and Fe species stability during the operation of HEF [38]. Fig. 8 shows the decrease of COD over time at different pH values for an operation time of 120 min at 10 mA/cm² and a catalyst dosage of 1.0 g/L. Fig. 9 shows the corresponding graph of $\ln(\text{COD}/\text{COD}_0)$ versus time. Similarly, the decrease in COD over time was found to follow an exponential behavior, and a straight-line relationship was observed for $\ln(\text{COD}/\text{COD}_0)$ with time, confirming the pseudo first-order kinetics of COD removal from PRW. The results show that increasing pH resulted in a decrease in COD removal and the rate constant, with both values decreasing significantly after pH 6. The high COD removal at pH 3 can be explained as follows: 1) the Fe and Ce loaded AC surface is prone to higher oxidation degree compared to higher pH leading to more $\cdot\text{OH}$ generation [37], 2) the oxidation capacity of $\cdot\text{OH}$ is affected by the pH of the solution and its oxidation

capacity is diminished at high pH values [65], 3) the increase in pH could result in a significant reduction in rate of in-situ generation of H₂O₂ [23], and 4) at high pH level, H₂O₂ is decomposed to O₂ rather than hydroxyl radicals [66]. Furthermore, the formation of Fe-OOH increases at higher pH leading to its precipitation on the catalyst surface causing a negative effect on $\cdot\text{OH}$ generation [67]. Finally, with increasing pH, the resulting iron-proxy complex as an intermediate in the Fenton reaction became more stable leading to less generation of $\cdot\text{OH}$ [68].

Table 5 shows the K_{app} value at different pH levels, with the corresponding R^2 values exceeding 0.979. At pH 3, the K_{app} value was 0.0188538 min⁻¹, and it decreased to 0.01738 min⁻¹ at pH 6, resulting in an 8.4% decrease. Furthermore, the K_{app} value decreased by 29% as the pH increased from 6 to 9. Therefore, increasing the pH above 6 reduces the reaction rate, which makes it advisable not to continue the reaction in terms of performance. The above results confirmed the ability to conduct HEF in a wide pH range to reach neutrality which cannot be

achieved using conventional homogeneous electro-Fenton technique. Table 5 shows that increasing the pH has a slightly effect on electrical energy consumption.

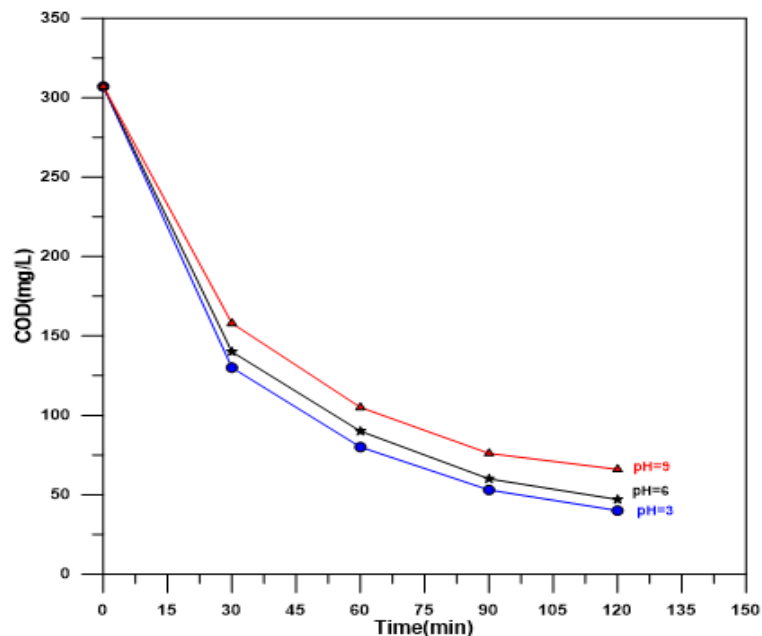


Fig. 8. Effect of pH on the COD removal in HEF

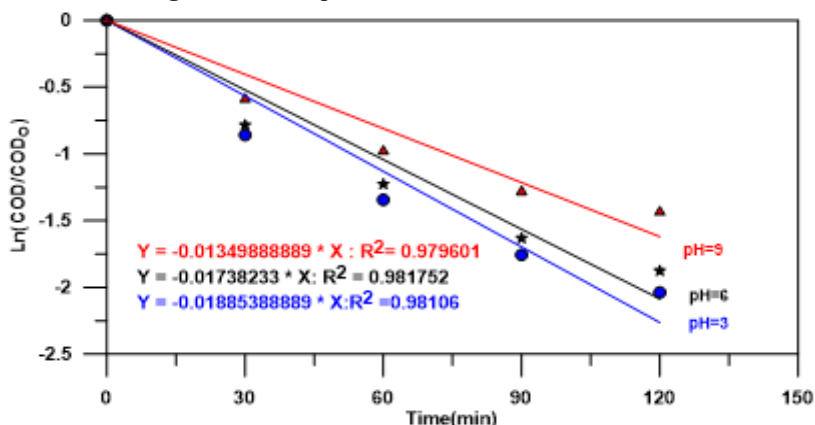


Fig. 9. Pseudo-first order kinetics for different pH at HEF. 1g/L catalyst, 10 mA/cm²

Table 5. Apparent rate constant at different pH

pH	Final COD ppm	RE%	SEC (KWh/ kg COD)	K _{app.} (min ⁻¹)	R ²
3	40	86.97	13.06	0.0188538	0.98106
6	47	84.50	13.38	0.017382	0.98175
9	66	78.50	15.336	0.013499	0.97960

Previous work has shown different trends, but all confirmed that pH 3 had the highest removal rate and high-rate constant. Tesnim et al. [38] found that increasing pH from 3 to 9 resulted in a decrease in the pseudo-first order rate constant from 1.73 to 0.308 min⁻¹, however, the decrease was 30% with increasing pH from 3 to 5 compared to 82% with increasing pH from 3 to 9 during the treatment of wastewater containing an antipyrine via HEF using AC-NZVI. Xu et al. [23] found that the pseudo-first order rate constant decreased from

0.0112/s at pH 3 to 0.0086/s at pH 6 during the treatment of a polyacrylamide pollutant using HEF. However, they found that the removal rate at pH 5 was still high at 79.63% when compared to the homogeneous Fenton electrolyte, which showed a significant decrease in the removal rate to 45.56%, confirming that HEF has better pH adaptability.

Tan et al. [48] observed that the rate constant at pH 5 was 0.12 min⁻¹, which is much higher than at pH 7 (0.0488 min⁻¹) and at pH 9 (0.0374 min⁻¹), but slightly

lower than at pH 3 (0.1344 min^{-1}) during the treatment of rhodamine B by HEF using calcined nanopyrite. Their results are consistent with ours. Sadeghi et al. [52] also observed a similar behavior during the degradation of diclofenac by HEF using a catalyst made of magnetic single-walled carbon nanotubes. In contrast, Pormazar and Dalvand [41] found no significant effect of pH on DB80 dye removal between pH 3 and 7 in its decomposition using HEF with magnetite-loaded AC Fe_3O_4 and DB80 dye removal decreased slightly at pH 9.

4- Conclusion

The kinetics of HEF process with iron and cerium-loaded AC during petroleum refinery wastewater treatment were successfully investigated. Effects of HEF operating variables such as current density, catalyst dosage, and pH on COD removal and the reaction rate constant (k_{app}) were examined. The kinetic study confirmed that the process follows a pseudo-first-order kinetic model under different operating variables studied in the present work with R^2 higher than 0.97. It was found that the COD removal and the reaction rate constant (k_{app}) increased with increasing current density up to 10 mA/cm^2 and increasing catalyst dosage up to 1 g/L . The effect of pH was significant as pH exceeded 6, and good COD removal and a suitable k_{app} value could be maintained in the pH range between 3 and 6, confirming that the present system has better pH adaptability. High COD removal rate and k_{app} could be attained at a current density of 10 mA/cm^2 , a catalyst dosage of 1.0 g/L , and a pH of 3, where 86.97% of COD was removed with recording reaction rate constant of $0.0188538 \text{ min}^{-1}$. The present system is a promising HEF technology for wastewater treatment, with the potential to improve the degradation efficiency and reduce energy consumption. It is also a promising process for overcoming the drawbacks of the homogeneous wastewater treatment process used in the conventional refinery wastewater treatment.

Acknowledgment

The authors thank the employees of Chemical Engineering Department, University of Baghdad for their technical assistance. Because of it, the authors have been able to complete this study.

References

- [1] M.Jiad and A.Abbar and Z.Jabbar," Advanced treatment of petroleum refinery wastewater by electro-Fenton and photo-catalytic processes," *Environmental Technology Reviews*, Vol. 14, 2025, pp.400-426.
<https://doi.org/10.1080/21622515.2025.2479713>
- [2] S.Jafarinejad and S.Jiang," Current technologies and future directions for treating petroleum refineries and petrochemical plants (PRPP) wastewaters," *Journal of Environmental Chemical Engineering*, Vol.7, 2019.
<https://doi.org/10.1016/j.jece.2019.103326>
- [3] N. Sadek and S. Alradhi and T. Albayati and I. Salih and N. Elmi," Recent developments in petroleum wastewater treatment based on advanced oxidation processes: a review," *Iranian Journal of Chemistry and Chemical Engineering*, Vol.44, 2025, pp.1089-1120.
<https://doi.org/10.30492/ijcce.2025.2044930.6870>
- [4] A. Merchant and A. Vakili Kocaman, A., & Amr, S. S. A.," New advancement of advanced oxidation processes for the treatment of Petroleum wastewater," *Desalination and Water Treatment*, 2024. <https://doi.org/10.1016/j.dwt.2024.100565>
- [5] I. Ousseini and M. Mounir and R. Kané," Current Approaches to Petroleum Wastewater Treatment for Reuse: A Systematic Review," *Journal of Materials and Environmental Science*, Vol.15, Dec. 2024, pp1814-1824.
- [6] Z. Atiyah and S. Muallah and A. Abbar," Removal of COD from petroleum refinery wastewater by adsorption using activated carbon derived from avocado plant," *South African Journal of Chemical Engineering*, Vol. 48, 2024, pp.467-483.
<https://doi.org/10.1016/j.sajce.2024.03.015>
- [7] B. Thorat, and R. Sonwani," Current technologies and future perspectives for the treatment of complex petroleum refinery wastewater: A review," *Bioresource Technology*, 2022.
<https://doi.org/10.1016/j.biortech.2022.127263>
- [8] M. Lawan, R. Kumar and J. Rashid, and M. Barakat," Recent advancements in the treatment of petroleum refinery wastewater," *Water*, Vol. 15, 2023.
<https://doi.org/10.3390/w15203676>
- [9] M. Ebrahimi and H. Kazemi and S. Mirbagheri, and T. Rockaway," An optimized biological approach for treatment of petroleum refinery wastewater," *Journal of environmental chemical engineering*, Vol.4, 2016, pp.3401-3408.
<https://doi.org/10.1016/j.jece.2016.06.030>
- [10] G.Rodrigus and V. Rezend and M.Cristina.," Applications and advancements in membrane technologies for sustainable petroleum refinery wastewater treatment," *Journal of Environmental Chemical Engineering*, Vol. 13, 2025, pp 115199.
<https://doi.org/10.1016/j.jece.2024.115199>
- [11] M.Arifin and R.Jusoh and H.Abdullah and N.Ainirazali and H.Setiabudi," Recent advances in advanced oxidation processes (AOPs) for the treatment of nitro-and alkyl-phenolic compounds," *Environmental research*, Vol. 229, 2023.
<https://doi.org/10.1016/j.envres.2023.115936>
- [12] M.Tony and P.Purcell and Y.Zhao," Oil refinery wastewater treatment using physicochemical, Fenton and Photo-Fenton oxidation processes," *Journal of Environmental Science and Health , Part A*, Vol. 47, 2012, pp.435-440.
<https://doi.org/10.1080/10934529.2012.646136>

- [13] M.Jiad and A.Abbar, "Treatment of petroleum refinery wastewater by sono fenton process utilizing the in-situ generated hydrogen peroxide," *Al-Khwarizmi Engineering Journal*, Vol.19, 2023, pp.52-67. <https://doi.org/10.22153/kej.2023.04.002>
- [14] Z.Khan and S.Sabahat and N.Shah and H.Ajab and J.Iqbal and F.Ullah," Electrochemical advanced oxidation processes as a feasible approach towards treatment of pesticides contaminated water and environmental sustainability: a review," *Journal of Water Process Engineering*, Vol.70, 2025. <https://doi.org/10.1016/j.jwpe.2025.107083>
- [15] P.Asaitamb and M.Yesuf and G. Rajendran and R., Hariharan and H. Mothilal," A Review of Hybrid Process Development Based on Electrochemical and Advanced Oxidation Processes for the Treatment of Industrial Wastewater," *International Journal of Chemical Engineering*, 2022. <https://doi.org/10.1155/2022/1105376>
- [16] J.D.García and J.Trevino and I.Robles and G.Acosta and L.A.Godínez," A review of electro-Fenton and ultrasound processes: towards a novel integrated technology for wastewater treatment," *Environmental Science and Pollution Research*, Vol.32, 2025, pp.10530-10552. <https://doi.org/10.1007/s11356-023-29877-9>
- [17] M.Jiad and A.Abbar," Treatment of petroleum refinery wastewater by an innovative electro-Fenton system: Performance and specific energy consumption evaluation," *Case Studies in Chemical and Environmental Engineering*, Vol.8, 2023 . <https://doi.org/10.1016/j.cscee.2023.100431>
- [18] M.Jiad and A.Abbar," Treatment of petroleum refinery wastewater by electrofenton process using a low cost porous graphite air-diffusion cathode with a novel design," *Chemical Engineering Research and Design*, Vol.193, 2023, pp. 207-221. <https://doi.org/10.1016/j.cherd.2023.03.021>
- [19] A.Salah and A. Abbar ,"Treatment of petroleum refinery wastewater by electro-Fenton process using porous graphite electrodes," *Egyptian Journal of Chemistry*, Vol.63, 2020, pp.4805-4819. <https://doi.org/10.21608/EJCHEM.2020.28148.2592>
- [20] G.Khaleel and I.Ismail and A. Abbar," Application of solar photo-electro-Fenton technology to petroleum refinery wastewater degradation: Optimization of operational parameters," *Heliyon*, Vol .9, 2023. <https://doi.org/10.1016/j.heliyon.2023.e15062>
- [21] Z.Hameed and R.Salman, "Elimination of methyl orange dye with three dimensional electro-Fenton and sono-electro-Fenton systems utilizing copper foam and activated carbon," *Ecological Engineering & Environmental Technology*, Vol.25, 2024. <https://doi.org/10.12912/27197050/191199>
- [22] H.Thwaini and R.Salman and W.Abdul-Majeed, "Performance of electro-Fenton process for phenol degradation using nickel foam as a cathode," *Iraqi Journal of Chemical and Petroleum Engineering*, Vol.24, 2023, pp.13-25. <https://doi.org/10.31699/IJCPE.2023.3.2>
- [23] S.Xu and Y.Yang and F.Li ,"Heterogeneous electro-Fenton removal of polyacrylamide in aqueous solution over CoFe₂O₄ catalyst," *Water Science & Technology*, Vol.89, 2024, pp.3309-3324. <https://doi.org/10.2166/wst.2024.180>
- [24] Z.Wang and M.Liu and F.Xiao and G.Postole and H.Zhao and G.Zhao,"Recent advances and trends of heterogeneous electro-Fenton process for wastewater treatment-review," *Chinese Chemical Letters*, Vol.33, 2022, pp. 653-662. <https://doi.org/10.1016/j.ccl.2021.07.044>
- [25] Y.Song and A.Wang and S.Ren and Y.Zhang and Z.Zhang, "Flow-through heterogeneous electro-Fenton system using a bifunctional FeOCl/carbon cloth/activated carbon fiber cathode for efficient degradation of trimethoprim at neutral pH," *Environmental Research*, Vol .222, 2023. <https://doi.org/10.1016/j.envres.2023.115303>
- [26] H.Liu and J.Jiang and L.Tang and Y.Liang and S.Xue, "Recent progress in electrocatalytic selectivity in heterogeneous electro-Fenton processes," *Journal of Materials Chemistry A*, Vol 11, 2023, pp. 7387-7408. <https://doi.org/10.1039/D2TA09676E>
- [27] Y.Zou and H.Qi and Z.Sun," In-situ catalytic degradation of sulfamethoxazole with efficient CuCo-O@ CNTs/NF cathode in a neutral electro-Fenton-like system," *Chemosphere*, Vol.296, 2022, 134072. <https://doi.org/10.1016/j.chemosphere.2022.134072>
- [28] C.Xue and Z.Cao and X. Tong and P.Yang, "Investigation of CuCoFe-LDH as an efficient and stable catalyst for the degradation of acetaminophen in heterogeneous electro-Fenton system: Key operating parameters, mechanisms and pathways," *Journal of Environmental Management*, Vol.327, 2023. <https://doi.org/10.1016/j.jenvman.2022.116787>
- [29] N.Barhoumi and H.Olvera-Vargas and N.Oturan and D. Huguenot and A.Gadri and S.Ammarand M.Oturan," Kinetics of oxidative degradation/mineralization pathways of the antibiotic tetracycline by the novel heterogeneous electro-Fenton process with solid catalyst chalcopyrite.," *Applied Catalysis B. Environmental*, Vol.209, 2017, pp. 637-647. <https://doi.org/10.1016/j.apcatb.2017.03.034>
- [30] Z.Ye and J.Padilla and E.Xuriguera and J.Beltran and F.Alcaide and E.Brillas," A highly stable metal-organic framework-engineered FeS₂/C nanocatalyst for heterogeneous electro-Fenton treatment: validation in wastewater at mild pH," *Environmental Science & Technology*, Vol.54, 2020, pp. 4664-4674. <https://doi.org/10.1021/acs.est.9b07604>

- [31] T.Luo and H.Feng and L.Tang and Y.Lu and W.Tang and S.Chen, "Efficient degradation of tetracycline by heterogeneous electro-Fenton process using Cu-doped Fe@ Fe₂O₃: Mechanism and degradation pathway," *Chemical Engineering Journal*, Vol.382, 2020. <https://doi.org/10.1016/j.cej.2019.122970>
- [32] C.Sánchez-Sánchez and E.Exposito and J.Casado and V.Montiel," Goethite as a more effective iron dosage source for mineralization of organic pollutants by electro-Fenton process," *Electrochemistry Communications*, Vol.9, 2007, pp. 19-24. <https://doi.org/10.1016/j.elecom.2006.08.023>
- [33] C.Zhang and F.Li and R.Wen and H.Zhang and P.Elumalai and Q.Zheng ,"Heterogeneous electro-Fenton using three-dimension NZVI-BC electrodes for degradation of neonicotinoid wastewater," *Water Research*, Vol. 182, 2020. <https://doi.org/10.1016/j.watres.2020.115975>
- [34] E.GilPavas and S.Correa-Sanchez ,"Optimization of the heterogeneous electro-Fenton process assisted by scrap zero-valent iron for treating textile wastewater: Assessment of toxicity and biodegradability," *Journal of Water Process Engineering*, Vol.32, 2019. <https://doi.org/10.1016/j.jwpe.2019.100924>
- [35] J.Guo and G.Song and X.Zhang and M.Zhou, "Transition metal catalysts in the heterogeneous electro-Fenton process for organic wastewater treatment: a review ,"*Environmental Science: Water Research & Technology*, Vol.9, 2023, pp 2429-2445. <https://doi.org/10.1039/D3EW00302G>
- [36] P.Nidheesh and R.Gandhimathi ,"Comparative Removal of Rhodamine B from Aqueous Solution by Electro-F enton and Electro-F enton-L ize Processes," *Clean Soil Air Water*, Vol. 42, 2014, pp. 779-784. <https://doi.org/10.1002/clen.201300093>
- [37] Y.Chen and L.Yang and J.Chenand Y.Zheng," Electrospun spongy zero-valent iron as excellent electro-Fenton catalyst for enhanced sulfathiazole removal by a combination of adsorption and electro-catalytic oxidation," *Journal of hazardous materials*, Vol.371, 2019, pp.576-585. <https://doi.org/10.1016/j.jhazmat.2019.03.043>
- [38] D.Tesnim and A.Diez and B.Hedi and M.Sanroman and M.Pazos,"Sustainable removal of antipyrine from wastewater via an Eco-Friendly heterogeneous Electro-Fenton-like process employing Zero-Valent iron nanoparticles loaded activated carbon," *Chemical Engineering Journal*, Vol.493, 2024. <https://doi.org/10.1016/j.cej.2024.152494>
- [39] Y.Lu and M.Feng and Y.Wang," Enhancing the heterogeneous electro-Fenton degradation of methylene blue using sludge-derived biochar-loaded nano zero-valent iron," *Journal of Water Process Engineering*, Vol.59, 2024. <https://doi.org/10.1016/j.jwpe.2024.104980>
- [40] A.Das and L.Chen," A review on electrochemical advanced oxidation treatment of dairy wastewater," *Environments*, Vol. 11, 2024. <https://doi.org/10.3390/environments11060124>
- [41] S.Pormazar and A.Dalvand, "Heterogeneous electro-Fenton process using a novel catalytic electrode for the degradation of direct dye from aqueous solutions: modeling, optimization, degradation pathway and toxicity evaluation," *Applied Water Science*, Vol.15, 2025. <https://doi.org/10.1007/s13201-025-02394-5>
- [42] D.Tesnim and A.Diez and H.Amor and M.Sanroman and M.Pazos," Synthesis and characterization of eco-friendly cathodic electrodes incorporating nano Zero-Valent iron (NZVI) for the electro-fenton treatment of pharmaceutical wastewater," *Chemical Engineering Journal*, Vol.502, 2024. <https://doi.org/10.1016/j.cej.2024.158099>
- [43] M.Dolatabadi and M.Ghaneian and C.Wang and S.Ahmadzadeh, "Electro-Fenton approach for highly efficient degradation of the herbicide 2,4-dichlorophenoxyacetic acid from agricultural wastewater: Process optimization, kinetic and mechanism," *Journal of Molecular Liquids*, Vol. 334, 2021. <https://doi.org/10.1016/j.molliq.2021.116116>
- [44] A.Shokri," A kinetic study and application of electro-Fenton process for the remediation of aqueous environment containing toluene in a batch reactor," *Russian Journal of Applied Chemistry*, Vol.90, 2017, pp. 452-457. <https://doi.org/10.1134/S1070427217030193>
- [45] A.Dirany and I.Sirés and N.Oturan and A.Özcan," Electrochemical treatment of the antibiotic sulfachloropyridazine: kinetics, reaction pathways, and toxicity evolution," *Environmental science & technology*, Vol. 46, 2012, pp. 4074-4082. <https://doi.org/10.1021/es204621q>
- [46] Y.Samet and I.Wali and R.Abelhédi ,"Kinetic degradation of the pollutant guaiacol by dark Fenton and solar photo-Fenton processes," *Environmental Science and Pollution Research*, Vol.18, 2011, pp.1497-1507. <https://doi.org/10.1007/s11356-011-0514-4>
- [47] H.Öztürk and S.Barıřçı and O.Turkay," Paracetamol degradation and kinetics by advanced oxidation processes (AOPs): Electro-peroxone, ozonation, goethite catalyzed electro-fenton and electro-oxidation," *Environmental Engineering Research*, Vol. 26, 2021. <https://doi.org/10.4491/eer.2018.332>
- [48] Y.Tan and C.Zhao and Q.Chen and L.Li and X.Wang, "Heterogeneous Electro-Fenton-Catalyzed Degradation of Rhodamine B by Nano-Calcined Pyrite," *International Journal of Environmental Research and Public Health*, Vol.20, 2023. <https://doi.org/10.3390/ijerph20064883>
- [49] L.Fan and X.Wang and J.Miao and J.Cai and F.Chen and W.Chen, "Core-shell structured Fe0/Mn0@ Fe/Mn oxides bimetallic nanocomposites as novel heterogeneous electro-Fenton catalysts for methylene blue removal," *Journal of Molecular Liquids*, Vol.383, 2023. <https://doi.org/10.1016/j.molliq.2023.122069>

- [50] D.Shang and W.Zheng and P.Zhao and Y.Li and L. Xie and J. Zhang, "Investigation on the reaction kinetic mechanism of polydopamine-loaded copper as dual-functional catalyst in heterogeneous electro-Fenton process," *Chemosphere*, Vol. 325, 2023. <https://doi.org/10.1016/j.chemosphere.2023.138339>
- [51] S.Campos and R.Salazar and N.Arancibia-Miranda and M. Rubio and M. Aranda and A.García," Nafcillin degradation by heterogeneous electro-Fenton process using Fe, Cu and Fe/Cu nanoparticles," *Chemosphere*, Vol.247, 2020. <https://doi.org/10.1016/j.chemosphere.2020.125813>
- [52] M.Sadeghi and M.Mehdinejad and N.Mengelizadeh and Y.Mahdavi and H.Pourzamani and Y.Hajizadeh," Degradation of diclofenac by heterogeneous electro-Fenton process using magnetic single-walled carbon nanotubes as a catalyst," *Journal of Water Process Engineering*, Vol. 31, 2019. <https://doi.org/10.1016/j.jwpe.2019.100852>
- [53] L.Bounab and O.Iglesias and E.González-Romero and M.Pazos and M.Sanromán ,"Effective heterogeneous electro-Fenton process of m-cresol with iron loaded activated carbon," *RSC Advances*, Vol. 5, 2015, pp. 31049-31056. <https://doi.org/10.1039/c5ra03050a>
- [54] L.Xu and J.Wang,"Magnetic nanoscaled Fe₃O₄/CeO₂ composite as an efficient Fenton-like heterogeneous catalyst for degradation of 4-chlorophenol," *Environmental science & technology*, Vol.46, 2012, pp.10145-10153. <https://doi.org/10.1021/es300303f>
- [55] Y.Raji and A.Nadi and I.Mechnou and M.Saadouni and O.Cherkaoui and S.Zyade," High adsorption capacities of crystal violet dye by low-cost activated carbon prepared from Moroccan Moringa oleifera wastes: Characterization, adsorption and mechanism study," *Diamond and Related Materials*, Vol. 135, 2023. <https://doi.org/10.1016/j.diamond.2023.109834>
- [56] X.Ling and J.Li and W.Zhu and Y.Zhu and X.Sun and J.Shen,"Synthesis of nanoscale zero-valent iron/ordered mesoporous carbon for adsorption and synergistic reduction of nitrobenzene," *Chemosphere*, Vol.87, 2012, pp. 655-660. <https://doi.org/10.1016/j.chemosphere.2012.02.002>
- [57] I.Ali and A.fshinb and Y.Poureshgh and A.Azari and Y.Rashtbari and A.Feizizadeh and M.Fazlzadeh ,"Green preparation of activated carbon from pomegranate peel coated with zero-valent iron nanoparticles (nZVI) and isotherm and kinetic studies of amoxicillin removal in water," *Environmental Science and Pollution Research*, Vol.27, 2020, pp. 36732-36743. <https://doi.org/10.1007/s11356-020-09310-1>
- [58] H.Ahemad and G.Patil and Y.Aher and M.Malik and L.Sonawane and M.More and G.Jain ," Synthesis and characterization of CeO₂ nanoparticles using Plectranthus barbatus leaf extract and its CO gas sensing and antimicrobial activity," *Materials Letters*, Vol.379, 2025. <https://doi.org/10.1016/j.matlet.2024.137652>
- [59] D.Huang and J.Liu and J.Zhang and Z.Chen and Z.Zhou and B.Xu and M.Wang," Enhanced removal of florfenicol by distributing nanoscale zerovalent iron onto activated carbon: mechanism and toxicity evaluation," *Chemical Engineering Journal*, Vol. 479, 2024. <https://doi.org/10.1016/j.cej.2023.147938>
- [60] J.Xiao and Q.Yue and B.Gao and Y.Sun and J.Kong and Y.Gao and Y.Wang," Performance of activated carbon/nanoscale zero-valent iron for removal of trihalomethanes (THMs) at infinitesimal concentration in drinking water," *Chemical engineering journal*, Vol.253, 2014, pp. 63-72. <https://doi.org/10.1016/j.cej.2014.05.030>
- [61] P.Ma and H.Ma and A.Galia and S.Sabatino and O.Scialdone," Reduction of oxygen to H₂O₂ at carbon felt cathode in undivided cells. Effect of the ratio between the anode and the cathode surfaces and of other operative parameters," *Separation and Purification Technology*, Vol. 208, 2019, pp. 116-122. <https://doi.org/10.1016/j.seppur.2018.04.062>
- [62] W.Zhou and L.Rajic and L.Chen and K.Kou and Y.Ding and X.Meng and A.Alshwabkeh ,"Activated carbon as effective cathode material in iron-free Electro-Fenton process: Integrated H₂O₂ electrogeneration, activation, and pollutants adsorption," *Electrochimical acta*, Vol.296, 2019, pp. 317-326. <https://doi.org/10.1016/j.electacta.2018.11.052>
- [63] H.Lin and J.Wu and N.Oturan and H.Zhang and M.Oturan," Degradation of artificial sweetener saccharin in aqueous medium by electrochemically generated hydroxyl radicals," *Environmental Science and Pollution Research*, Vol.23, 2016, pp. 4442-4453. <https://doi.org/10.1007/s11356-015-5633-x>
- [64] N.Barhoumi and N.Oturan and H.Olvera-Vargas and E.Brillas and A.Gadri and S.Ammar " Pyrite as a sustainable catalyst in electro-Fenton process for improving oxidation of sulfamethazine. Kinetics, mechanism and toxicity assessment," *Water Research*, Vol.94, 2016, pp. 52-61. <https://doi.org/10.1016/j.watres.2016.02.042>
- [65] L.Feng and E.Serna-Galvis and N.Oturan and S.Giannakis and R.Torres-Palma and M.Oturan,"Evaluation of process influencing factors, degradation products, toxicity evolution and matrix-related effects during electro-Fenton removal of piroxicam from waters," *Journal of Environmental Chemical Engineering*, Vol.7, 2019. <https://doi.org/10.1016/j.jece.2019.103400>
- [66] X.Nie and G.Li and S.Li and Y.Luo and W.Luo and Q.Wan and T.An ,"Highly efficient adsorption and catalytic degradation of ciprofloxacin by a novel heterogeneous Fenton catalyst of hexapod-like pyrite nanosheets mineral clusters," *Applied Catalysis B: Environmental*, Vol.300, 2022. <https://doi.org/10.1016/j.apcatb.2021.120734>

- [67] J.Vialich and D.Sugai and F.Wypych and C.Benincá and E. Zanoelo ,”Electromigration of protons and zero valent iron oxidation: A physico-chemical insight to model the kinetics of fenton-like process,” *Chemical Engineering Journal*, Vol.435, 2022. <https://doi.org/10.1016/j.cej.2022.135026>
- [68] Y.Zhang and M.Yang and Z.Ling and Y.Liu and W.Wu,”FingerAuth: 3D magnetic finger motion pattern based implicit authentication for mobile devices,” *Future Generation Computer Systems*, Vol.108, 2020, pp. 1324-1337. <https://doi.org/10.1016/j.future.2018.02.006>

تحلل مياه الصرف الصحي لمصافي البترول بواسطة عملية إلكترو- فنتون غير المتجانسة باستخدام الكربون المنشط المحمل بالحديد والسيريوم: دراسة حركية

آسيه رماح فليح^{١*}، ودود طاهر محمد^١، علي حسين عبار^٢

^١ قسم الهندسة الكيميائية، كلية الهندسة، جامعة بغداد، بغداد ١٠٠٧١، العراق

^٢ قسم الهندسة الكيميائية الاحيائية، كلية الخوارزمي للهندسة، جامعة بغداد، بغداد ١٠٠٧١، العراق

الخلاصة

تهدف هذه الدراسة إلى بحث حركية التفاعل لعملية إلكترو- فنتون غير المتجانسة (HEF) والمستخدم في معالجة المياه العادمة الخارجة من مصافي البترول، وذلك باستخدام محفز مصنوع من الكربون المنشط المحمل بالحديد والسيريوم. تم فحص تأثير متغيرات تشغيل عملية HEF والمتمثلة بكثافة التيار، جرعة المحفز، ودرجة الحموضة، على إزالة الطلب الكيميائي للأكسجين (COD) وثابت معدل التفاعل (K_{app}). أظهرت النتائج أن انخفاض الطلب الكيميائي للأكسجين مع مرور الوقت في ظل ظروف تشغيل مختلفة يتبع حركية تفاعل من الرتبة الأولى الزائفة، بمعامل تحديد (R^2) لا يقل عن ٠.٩٧. علاوة على ذلك، وُجد أن زيادة كثافة التيار تؤدي إلى زيادة معدل إزالة الطلب الكيميائي للأكسجين وثابت معدل التفاعل (K_{app}) إلى حد معين بعده لا يوجد أي تحسين إضافي. لوحظ سلوك مماثل فيما يتعلق بجرعة المحفز، بينما كان لزيادة درجة الحموضة تأثير سلبي. كانت أفضل الظروف التشغيل التي حققت أعلى معدل إزالة الطلب الكيميائي للأكسجين (COD) بمقدار ٨٦.٩٧٪ واكبر قيمة لثابت معدل التفاعل (K_{app}) بمقدار ٠.٠١٨٨٥٣٨ دقيقة^{-١} هي كثافة تيار ١٠ ملي أمبير/سم^٢، وجرعة محفز ١.٠ غ/لتر، ودرجة حموضة ٣، حيث تطلب ذلك استهلاك طاقة كهربائية بمقدار ١٣.٠٦ كيلوواط ساعة/كغ من الأكسجين الكيميائي الحيوي. وقد أثبت النظام الحالي فعاليته في الحصول على معدل تفاعل عالي، ويمكن تطبيقه لمعالجة أنواع مختلفة من مياه الصرف الصحي.

الكلمات الدالة: مياه الصرف الصحي لمصفاة البترول، حركية من الدرجة الأولى الزائفة، إلكترو-فنتون غير المتجانس، عملية الأكسدة المتقدمة.